Journal of Animal Ecology

DR HUGO CAYUELA (Orcid ID : 0000-0002-3529-0736)

DR BLAKE HOSSACK (Orcid ID : 0000-0001-7456-9564)

Genomic signatures of thermal adaptation are associated with clinal shifts of life history in a broadly distributed frog

Hugo Cayuela[1], Yann Dorant[2], Brenna R. Forester[3], Dan L. Jeffries[1], Rebecca M. Mccaffery[4], Lisa A. Eby[5], Blake R. Hossack[6], Jérôme M. W. Gippet[1], David S. Pilliod[7], W. Chris Funk[3]

Affiliations

[1]Department of Ecology and Evolution, University of Lausanne, 1015 Lausanne, Switzerland

[2]Institut de Biologie Intégrative et des Systèmes (IBIS), Université Laval, Québec, QC, Canada

[3]Department of Biology, Graduate Degree Program in Ecology, Colorado State University, Fort Collins, CO, U.S.A.

[4]US Geological Survey, Forest and Rangeland Ecosystem Science Center, Port Angeles, WA, USA.

[5]Wildlife Biology Program, W. A. Franke College of Forestry and Conservation, University of Montana, Missoula, MT, U.S.A.

[6]US Geological Survey, Northern Rocky Mountain Science Center, Missoula, MT, USA and Wildlife Biology Program, W. A. Franke College of Forestry and Conservation, University of Montana, Missoula, MT, USA

[7]US Geological Survey, Forest and Rangeland Ecosystem Science Center, Boise, ID, U.S.A.

Corresponding author: Hugo Cayuela
Email: hugo.cayuela51@gmail.com

Abstract (350 words max.)

1. Temperature is a critical driver of ectotherm life history strategies, whereby a warmer environment is associated with increased growth, reduced longevity, and accelerated senescence. Increasing evidence indicates that thermal adaptation may underly such life history shifts in wild populations. Single Nucleotide Polymorphisms (SNPs) and Copy Number Variants (CNVs) can help uncover the molecular mechanisms of temperature-driven variation in growth, longevity, and senescence. However, our understanding of these mechanisms is still limited, which reduces our ability to predict the response of non-model ectotherms to global temperature change.

2. In this study, we examined the potential role of thermal adaptation in clinal shifts of life history traits (i.e., lifespan, senescence rate, and recruitment) in the Columbia spotted frog (*Rana luteiventris*) along a broad temperature gradient in the western USA.

3. We took advantage of extensive capture-recapture datasets of 20,033 marked individuals from eight populations surveyed annually for 14 – 18 years to examine how mean annual temperature and precipitation influenced demographic parameters (i.e., adult survival, lifespan, senescence rate, recruitment, and population growth). After showing that temperature was the main climatic predictor influencing demography, we used RAD-seq data (50,829 SNPs and 6,599 putative CNVs) generated for 352 individuals from 31 breeding sites to identify genomic signatures of thermal adaptation.

4. Our results showed that temperature was negatively associated with annual adult survival and reproductive lifespan and positively associated with senescence rate. By contrast, recruitment increased with temperature, promoting the long-term viability of most populations. These temperature-dependent demographic changes were associated with strong genomic signatures of thermal adaptation. We identified 148 SNP candidates associated with temperature including three SNPs located within protein-coding genes regulating resistance to cold and hypoxia, immunity, and reproduction in ranids. We also identified 39 CNV candidates (including within 38 transposable elements) for which normalized read depth was associated with temperature.

5. Our study indicates that both SNPs and structural variants are associated with temperature and could eventually be found to play a functional role in clinal shifts in senescence rate and life history strategies in *R. luteiventris*. These results highlight the potential role of different sources of molecular variation in the response of ectotherms to environmental temperature variation in the context of global warming.

Introduction

Global temperatures are projected to increase up to 4°C by the end of the current century (IPCC 2014), with dramatic consequences for the individual life history and long-term viability of animal populations (Stenseth & Mysterud 2002, Selwood et al. 2015, Walsh et al. 2019). The demographic impact of global warming is expected to be particularly severe in ectothermic animals that have limited capacities to use metabolic heat to maintain their body temperature, making their life history traits highly sensitive to temperature variation (Seebacher et al. 2015, Burraco et al. 2020). Studies on free-ranging and experimental populations have shown that warmer environmental temperatures decrease ectotherm longevity (Munch & Salinas 2009, Flouris & Piantoni 2015, Keil et al. 2015) and accelerate their actuarial senescence (i.e., increase in mortality with age; Valenzano et al. 2006, Jacobson et al. 2010, Yen & Mobbs 2010). In parallel, ectotherm growth and reproductive rate increase with temperature (Huey & Berrigan 2001, Angilletta et al. 2004, Burraco et al. 2020). Together, these temperature-dependent processes regulate the position of populations and species along the *fast-slow continuum* of life history (*sensu*, Promislow & Harvey 1990). In ectothermic vertebrates (e.g., fish: Blanck & Lamouroux 2007, amphibians: Morrison & Hero 2003), individuals from cold environments (at high altitude and latitude) have slower life history (i.e., reduced growth rate, delayed sexual maturity, low fecundity, and long adult lifespan) than those experiencing warmer conditions. The evolutionary mechanisms underlying these temperature-driven shifts in life history, however, are still poorly understood, which limits our ability to accurately predict the fate of ectotherm populations in the face of global warming (Mims et al. 2018).

For a long time, temperature-dependent changes in life history have been thought to be regulated by adaptive plasticity. Thermoregulatory behaviors indeed allow ectotherms to plastically adjust their body temperature and buffer the detrimental impact of thermal variation on survival (Gunderson & Stillman 2015, Bodensteiner et al. 2021). Furthermore, warm environments induce thermal plasticity in most ectotherms, resulting in fast growth at the expense of adult lifespan, possibly via the rapid accumulation of oxidative damage (Burraco et al. 2020). However, an increasing number of molecular studies suggests that temperature-driven changes in life history could be also partially regulated by thermal adaptation. Genotype-environment associations (GEA) have revealed molecular signals of thermal adaptation in a broad range of ectotherms by identifying Single Nucleotide Polymorphisms (SNPs) whose allelic frequencies are correlated with temperature (e.g., lacustrine and marine fishes: Perrier et al. 2017, Cayuela et al. 2020a; amphibians: Rödin-Mörch et al. 2019; reptiles: Rodríguez et al. 2017; crustaceans: Benestan et al. 2016; molluscs: Lehnert et al. 2019; insects: Parker et al. 2018). In addition, genome-wide association studies (GWAS) showed that SNPs were associated with changes in thermal preference (Campbell-Staton et al. 2020), thermal tolerance (i.e., survival in response

to thermal stress; Rajpurohit et al. 2018, Amish et al. 2019), cardiac performances (e.g., Chen & Narum 2021), growth rate (Quigley et al. 2020), and mitochondrial metabolism (Mallard et al. 2018) among ectotherm populations experiencing contrasting temperature conditions.

Genomic structural variation (Wellenreuther et al. 2019, Mérot et al. 2020) could also contribute to the thermal adaptation underlying temperature-dependent changes of life history. Copy Number Variants (CNVs) are structural variants in which a segment of DNA can be absent or present in two or more paralogous copies (in diploid species) due to either gene duplication, deletion, or transposable elements (TEs) (Mérot et al. 2020). Studies have identified molecular signatures of adaptation involving CNVs (i.e., including duplicated coding and regulatory regions) whose copy number covaried with local temperature in marine fish and crustaceans (Dorant et al. 2020, Cayuela et al. 2021). Furthermore, interspecific comparisons between the long-lived Antarctic toothfish and its short-lived relatives from warm water identified dozens of genes in multiple copies that were overexpressed and likely improved survival and growth of toothfish in cold and oxygen-rich waters of the Antarctic zone (Chen et al. 2008). In addition, thermal stress experienced during an individual's lifetime may lead to temperature-dependent accumulation of TEs (Carducci et al. 2020), which are known to generate a broad variety of mutations that may lead to phenotypic and fitness variation through the modification of gene expression, the inactivation of genes, and the alteration of gene sequence and reading frame (Casacuberta & González 2013, Chuong et al. 2017).

To date, few studies have investigated whether life history and senescence acceleration driven by temperature are associated with molecular signatures of thermal adaptation among wild ectotherm populations. Here, we address this issue in the Columbia spotted frog (*Rana luteiventris*), a pond-breeding anuran from the western United States and Canada that is threatened by increasing environmental temperatures and decreasing precipitation during its active season (April to October) (Pilliod et al. 2015), particularly in the southern end of its distribution where drought is increasingly prevalent (Pilliod et al. 2021). This species is an excellent model for our study because it is widely distributed (distribution range size: 1,322,432 km2, encompassing parts of eight U.S. states and two Canadian provinces) and its populations are spread along a broad gradient of mean annual temperature (ranging from 1.71 to 8.35°C in our study area). Taking advantage of long-term (from 14 to 18 years, depending on site) capture-recapture data collected in eight populations of *R. luteiventris* in the United States (**Fig.1**), we tested the hypothesis that senescence rate increases with mean annual temperature while adult survival and longevity decrease. Furthermore, we predicted that recruitment increases with mean annual temperature, leading to an acceleration of life history strategies along the thermal gradient. Then, generating RAD-seq data from DNA samples collected across 31 breeding sites (**Fig.1**), we examined SNP-temperature and CNV-temperature associations to detect genomic signatures of thermal adaptation and to

identify candidate genes that might be involved in the life history shifts detected using demographic analyses. In light of these analyses, we then discuss the potential role of adaptation in life history shifts and an organism's response to global warming.

Materials and methods

Demographic analyses

Capture-recapture data collection

We collected capture-recapture data at eight populations or metapopulations from four states within the range of *R. luteiventris* in the western United States (**Fig.1**). The survey period differed among populations, ranging from 14 to 18 years (see detailed information in **Supplementary material, Table S1**). The surveyed populations were generally spread across multiple breeding waterbodies, thus behaving like "metapopulations" (*sensu lato*). The studied populations were generally not selected randomly, but represent a convenient and opportunistic sample of *R. luteiventris* populations. Populations were typically large enough to conduct mark-recapture studies, conveniently located for researchers and workers, and relatively free from major anthropogenic threats.

This study focused on adult frogs (with a snout-vent length longer than 45 mm) that were captured during annual visual encounter surveys. Surveys were conducted during a consistent 1–3 week period each year (usually July or August), depending on the studied population. For each population, wetland surveys consisted of 1-8 workers searching for animals along the shoreline of deeper water bodies or the entire surface area of wadable water bodies. Most populations were surveyed 2-3 times during this annual survey period to increase capture rates. Frogs were surveyed during the day when air temperatures were above 10 C. Sampling was time-constrained whereby surveys ended either when the entire area was thoroughly searched or about 30 min after the last animal was captured.

All captured animals were checked for an individual mark or tagged if they were unmarked. Unmarked individuals were injected with a passive integrated transponder (PIT) tag into the dorsal subcutaneous tissue or marked with a unique pattern of toeclips (Montana population only, prior to 2013). The PIT tag number of all newly marked animals as well as all recaptured individuals was recorded. After handling, frogs were released approximately at the location where they were captured or at least within the same water body, and always with minutes or an hour of capture. The number of individual frogs marked per population ranged from 370 in

population POCR to 8215 in population TOIY (Supplementary material S1, Tables S1). The number of captures ranged from 707 in population GRMO to 13,067 in population TOIY.

Climate data were compiled from 800-m Parameter-elevation Relationships on Independent Slopes Model [PRISM] Climate Group, Oregon State University, http://prism.oregonstate.edu, accessed 5 October 2020). For the 30-year period, 1990 – 2019, we calculated the mean and standard deviation of annual temperature, and the mean and standard deviation of annual cumulative precipitation for each population. Because populations occupied complex waterbody networks spread across sometimes large areas (e.g., lakes within mountain basins or several km of stream), we selected the coordinates of the area of highest animal density to use for our modeled climate data.

Estimating adult survival, seniority, and population growth rate

We estimated adult survival (φ), seniority (γ), and population growth rate (λ) for the eight populations using the Bayesian formulation of the Pradel model (Pradel 1996) proposed by Tenan et al. (2014). Seniority probability is the probability that, at each year y, an individual was already present in the population at y-1; hence, 1-γ corresponds to the probability that an individual was recruited in the population between y-1 and y (Pradel 1996). Population was assumed to be stable if $\lambda = 1$, to experience a decline if $\lambda < 1$, or to be growing if λ was > 1. We included a random effect of year on those three parameters to quantify their temporal variance. As the number of study years differed among populations, the eight populations were analyzed separately. Summaries of posterior parameter distributions were calculated from three independent Markov chains of 1 000 000 iterations initialized with random starting values, run 500 000 times after a 50 000 burn-in and resampling every 20 draws. We evaluated chain convergence using the R package Coda (Plummer et al. 2006). The models were implemented in program JAGS (Plummer 2003), that we executed from R (R Core Team 2019) with the package R2 JAGS (Su & Yajima 2012).

Estimating senescence rate and lifespan

Senescence rate and adult lifespan were calculated using the modeling procedure proposed by Lemaître et al. (2020). Bayesian survival trajectory analyses implemented in the R package BaSTA were used to estimate those mortality metrics (Colchero & Clark 2012, Colchero et al. 2012). Simulations by Colchero & Clark (2012) showed that BaSTA models are highly efficient to investigate age-dependent mortality when dates of birth and death are unknown and recapture probability is imperfect. BaSTA therefore allowed us to account for imperfect detection, left-truncated (i.e., unknown birth date (age)) and right-censored (i.e., unknown death date) capture-recapture data in our analysis. Again, the eight populations were analyzed separately. In an effort

to be conservative, we specified time-dependent recapture probability for all species. Four MCMC chains were run with 50000 iterations and a burn-in of 5000. Chains were thinned by a factor of 50. Model convergence was evaluated using the diagnostic analyses implemented in BaSTA, which calculate the potential scale reduction for each parameter to assess convergence.

We fitted a Siler model on age-specific mortality data (Siler 1979) for each species to obtain comparable metrics. The five-parameter Siler model is given by:

$$\mu(x) = a_0 exp(-a_1 x) + c + b_0 exp(b_1 x)$$

where a_0, a_1, b_0, b_1 and $c \geq 0$ are the parameters of the mortality function and x the age in years. The first exponential function with parameters a describes mortality in early adult stage, whereas c gives the lower limit of mortality during the adult stage. The second exponential function with b parameters corresponds to the mortality increase during the senescent stage. The parameter b_1 of the Siler model measures the exponential increase in mortality rate with age, and is therefore commonly used as a metric of rate of mortality aging in vertebrates (Lemaître et al. 2020, Ronget & Gaillard 2020).

Following the procedure presented in Lemaître et al. (2020), we estimated adult lifespan 80% (in years), corresponding to the age at which 80% of the individuals alive at the onset of adulthood (i.e., when first reproduction occurs) were dead (i.e., when cumulative survivorship reaches 0.8). Adult lifespan 80% was calculated from Siler model parameters by solving numerically the following equation:

$$e^{\left(\frac{a_0}{a1}(e^{-a_1 x} - 1) - cx + \frac{b_0}{b_1}(1 - e^{-b_1 x})\right)} = 0.8$$

Statistical analyses

We used linear models to examine the effect of mean temperature and precipitation (calculated for the period 1990-2019) on aging rate, lifespan 80%, mean annual adult survival, mean annual seniority, seniority, and mean annual population growth rate. The demographic parameters were included as response variables (log-transformed) whereas the climate variables were included as explanatory variables. The effect of the temperature and precipitation were examined separately. We used likelihood ratio tests performed between the models with and without the climatic covariate to assess the significance of the relationships. R^2 were also calculated. Furthermore, we used a similar approach to investigate the effect of temporal variability of temperature and precipitation (standard deviation calculated for the period 1990-2019) on the temporal variance (standard deviation) of annual adult survival, seniority, and population growth rate. Siler model parameters appropriately converged for all populations except POCR; hence, aging rate and lifespan 80% of this population were not included in the analyses.

Molecular analyses

Sampling area and DNA collection

Toe clips (from metamorph and adult frogs) and tail clips (5-10 mm, from tadpoles) were collected between 2010-2019. Individuals were captured at 31 breeding ponds across the Nevada range (**Fig.1**). The ponds were located within 10 hydrographic catchments (**Fig.1**). All individuals were released at their capture location after processing. The average number of individuals sampled in the breeding ponds was 11 (range: 4-14) (see **Supplementary material S1**, **Table S2** for sampling, geographical, and temperature information).

DNA extraction, library preparation and RAD-sequencing

We extracted DNA from tissue samples using Qiagen DNeasy Blood and Tissue Kits following manufacturer protocols, with the addition of 4 µl of RNase after tissue digestion. We quantified total DNA concentrations using Qubit dsDNA BR Assays and verified DNA quality in a subset of individuals using electrophoresis on agarose gels.

We tested five restriction enzyme digestions on a subset of individuals to find the enzyme combination that provided the appropriate distribution of fragment sizes (250-450 base pairs). We then digested ~1μg of total DNA per individual using *NspI* and *Eco-RI*. We followed Peterson et al. (2012), using a Pippin Prep size selection of 346-456 base pairs and Dynabeads cleanup. We used KAPA HiFi Hotstart Ready Mix for PCR amplification, and degenerate barcodes on the P2 adapter to facilitate removal of PCR duplicates (Schweyen et al. 2014). We sequenced one library with the University of Oregon Genomics Core Facility (HiSeq-4000, 100 bp paired-end reads), and the remaining nine libraries with Novogene Corp. (HiSeq-4000 150 bp paired-end reads). The first two libraries contained 24 and 36 individuals, respectively. All remaining libraries contained 40 individuals. Sites were split across libraries to avoid confounding site and library effects.

We used FastQC v. 0.11.8 (Andrews 2019) to assess data quality and identify sequencing anomalies in each library. We removed PCR duplicates from the raw reads using clone_filter from Stacks v. 2.41 (Catchen et al. 2011, 2013; Rochette et al. 2019). Using Trim Galore! v. 0.6.4 (Krueger 2019) and Cutadapt v. 2.5 (Martin 2011), we removed the 10 bp degenerative barcodes from the P2 reads and applied quality screening using a Phred score cutoff of 20 and auto-detect adapter screening with stringency set to 6. We then used Stacks process_radtags to demultiplex the raw data, trim reads to 90 bp, and run additional quality control

(remove reads with an uncalled base; discard reads with low quality scores (default settings); rescue barcodes and cut sites with at most one mismatch).

We used within and cross-library replicates to optimize three de novo Stacks parameters: minimum stack depth (-m), distance between stacks (-M), and the distance between catalog loci (-n). We used 19 individuals, each with a replicate sample, from 16 sites (total samples = 38), covering the geographic range of sampling effort. Thirteen combinations of -m (3-5), -M (2-6), and -n (1-6) were tested across the entire pipeline, setting the upper bound on the error rate for the SNP model (ustacks --bound-high) to 0.05. To determine the optimal combination of parameters, we evaluated mean coverage, the number of assembled loci, the number of polymorphic loci shared across 80% of individuals, and the number of SNPs (Paris et al. 2017). We also assessed population/duplicate clustering in multivariate space using multidimensional scaling plots (Gugger et al. 2018) calculated in plink v. 1.90 (Chang et al. 2015).

After optimizing Stacks parameters, we ran the Stacks pipeline on all unique samples and filtered using the populations module: -p 1 (minimum number of populations a locus must be present in to process), -R 0.3 (minimum percentage of individuals across populations required to process a locus), --min_mac 2 (minimum minor allele count required to process a SNP). We then ran the 'populations' module from Stacks to produce a vcf file defining the minimum number of populations a locus must be present in to process (p=1), the minimum percentage of individuals across populations required to process a locus (R=0.3), and the minimum minor allele count required to process a SNP (min_mac 2). The outputed vcf file was further filtered using python and bash scripts from the *stacks workflow* RADseq pipeline analysis available online (https://github.com/enormandeau/stacks_workflow). The raw vcf was filtered keeping only SNPs that showed a minimum coverage depth of 10x, were called in at least 70% of the samples per sampling location (according a maximum of four locations that can fail this latter filter) and a minimum number of samples having the rare allele of four across all sampling locations. Ultimately, samples showing more than 60% of missing data and SNPs showing more than 40% of missing data were discarded.

SNP and CNV discovery

We discriminated SNPs and putative CNVs using the *HDplot* approach initially proposed by McKinney et al. (2017) and recently adapted to CNV studies by Dorant et al. (2020) and Cayuela (2021). The duplicated loci detected by this method can be variant or invariant in copy number among the studied populations. A duplicated locus is considered as a CNV only if a correlation between the normalized read depth of a marker and a phenotypic trait or an environmental variable is detected. For this reason, we systematically use the term of "putative CNVs" when we refer to the markers identified using the *HDplot* method.

The *HDplot* approach extended by Dorant et al. (2020) discriminates "singleton" SNPs (i.e., non-duplicated) from "duplicated" SNPs (i.e., combining duplicated and diverged SNPs and SNPs with a high coverage) using four parameters: (1) proportion of heterozygotes (PropHet), (2) inbreeding coefficient - Fis, (3) median of allele ratio for heterozygotes (MedRatio), and (4) proportion of rare homozygotes. The parameters were calculated using a custom python script (available at https://github.com/enormandeau/stacks_workflow) parsing the filtered VCF file. The four parameters were plotted pairwise to visualize their distribution across all loci (see **Supplementary material**, **Fig.S1**). Based on the graphical demonstration by McKinney et al (2017), we considered different combinations of parameters and graphically fixed the cut-off of the five categories of SNPs (singleton SNPs, duplicated SNPs, diverged SNPs, high coverage SNPs, and low confidence). We then kept all RAD loci associated with either duplicated, diverged and high-coverage categories and extracted the loci read depth of to construct the dataset of putative CNVs using vcftools. For more simplicity, the term "putative CNV" is used to define all loci classified as "duplicated", "diverged" and "high coverage".

Following the procedure described in Dorant et al. (2020) and Cayuela et al. (2021), read counts of putative CNV loci were normalized to account for differences in sequencing effort across all samples. Normalization was performed using the Trimmed mean of M-values method originally described for RNA-seq count normalization and implemented in the R package edgeR (Robinson & Oshlack 2010). The correction accounts for the fact that for an individual with a higher copy number at a given locus, that locus will contribute proportionally more to the sequencing library than it will for an individual with lower copy number at that locus.

Finally, two separated datasets were generated; the "SNP data set", composed by singletons SNP only and the "CNV data set", which is the matrix of normalized read depth described above. To construct the SNP data set, we conserved the genotype calls from the VCF containing singleton SNPs, and postfiltered these by keeping all unlinked SNPs within each locus using the python script *11_extract_unlinked_snps.py* available in *stacks workflow*. Briefly, linkage was assessed for each pair of SNPs considering samples without missing data where at least one of the two genotypes contains the rare allele. If the two SNPs had identical genotypes in more than 30% among samples, the pair was considered linked and only the first SNPs was kept.

Putative CNVs and DNA repeats in ranids

A previous study using similar RAD-seq based CNV analyses showed that putative CNVs often correspond to DNA repeats (Cayuela et al. 2021). Therefore, we investigated the proportion of CNVs which fell into DNA repeats, relative to non-CNV RADtags. In addition, we examined if DNA repeats detected as putative CNVs

diverged more recently than the other elements of their own repeat family located in the rest of the genome by analyzing the relative age of their sequences.

We used RepeatMasker v.4.0.7 (Smit et al. 2015) to search RAD tag sequences against the custom repeat library which exists for the unpublished *R. temporaria* genome assembly (available at https://github.com/DanJeffries/Rana-temporaria-genome-assembly/wiki). To reduce computational complexity, we randomly selected 5 subsets of 10,000 RADtags from the full catalog to act as a baseline expectation for a given set of RAD tags in the dataset. For each subset, we examined the proportion of tags that were assigned to each repeat family, and the relative age of the repeat sequences (Kimura distance). We then did the same for 6,599 sequences identified as putative CNVs and for 39 sequences identified as candidate CNVs associated with temperature (see Results section). All five subsets of randomly selected RAD tags were almost identical in their proportions and TE age landscapes and were thus combined and used for comparisons with the CNV set. The proportions of RAD tags falling into each major repeat family (DNA transposons, LTR retransposons, and Miniature Inverted-repeat Transposable Elements (MITEs); Bourque et al. 2018) were compared between the baseline and CNV subsets using Fisher's exact test. The distributions of TE age were compared for each minor TE family (DNA/DTA, DNA/DTC, DNA/DTH, DNA/DTM, DNA/DTT, DNA/Helitron, LTR/Copia, LTR/Gypsy, LTR/unknown, MITE/DTA, MITE/DTC, MITE/DTH, MITE/DTM, MITE/DTT) separately using Welch's t-test for equal means, and Kolmogorov–Smirnov test. All statistical tests were implemented in Scipy v.1.5.1 in Python 3.6.3.

SNP-temperature associations

From our 50,829 SNPs singletons (see Results section), we first examined population genetic structure using a Principal Component Analysis (PCA) and level of genetic differentiation among sampling locations. We also calculated pairwise F_{ST} using the R library StAMPP (Pembleton et al. 2013) with 95% CI estimated on 1,000 bootstraps.

Following the recommendations of Forester et al. (2018), SNP-temperature associations were then evaluated using a combination of latent factor mixed models (LFMM; Frichot et al. 2013) and partial redundancy analysis (pRDA, Legendre & Legendre 2012) to detect SNP candidates. To minimize the number of false positives, we corrected for population genetic structure in LFMMs (Forester et al. 2018). In the pRDA, we controlled for sequencing libraries to control for the potential bias caused by batch effect that we detected within the genomic data (see **Supplementary material**, **Figure S7**). Next, we retained the outliers that were detected by both methods, and we represented the overlap with a Venn diagram. In the pRDA, an analysis of variance (ANOVA) with 1,000 permutations was performed to assess the significance of the model. SNPs

candidates were identified as those exhibiting a loading greater than 2.25 standard deviations from the mean loading (P < 0.025). We tested for linear correlations between allele frequencies and mean annual temperature using latent factor mixed models implemented in the R package LFMM 2 (Caye et al. 2019). We first performed a principal component analysis (PCA) and assessed the global population structure in the genotypic data. After determining how many components (K) explained most of the genotypic variance, genomic inflation factors (λ) were processed with the function *lfmm_ridge* and *z* scores were calculated with the function *lfmm_test*. Resulted *p*-values were adjusted based on λ and the χ^2 distribution (Caye et al. 2019). To control for false positives, we also applied a Benjamini-Hochberg correction algorithm with a false discovery rate (FDR) of 0.01 (Benjamini & Hochberg 1995). To reduce the number of false positives and correct our GEA for both batch effect and population structure, we only retained the candidate SNPs that were detected by both LMMs and pRDA and represented the overlap with a Venn diagram. Then, to identify potential candidate genes involved in thermal adaptation, we performed BLAST analyses for the locus sequences bearing candidate SNPs against the NCBI NR database. To consider a SNP further, we required a blast length of at least 80 bp and an e-value of 1e-10.

CNV-temperature associations

CNV-temperature associations were evaluated by combining locus-by-locus regressions and multivariate analyses following the approach used in Dorant et al. (2020) and Cayuela et al. (2021). First, we used a partial redundancy analysis to detect CNV candidates that were associated with temperature after controlling for a sequencing batch effect detected with a PCA performed on the normalized read depth matrix (**Supplementary material**, **Fig.S2**). Global and marginal analyses of variance (ANOVA) with 1,000 permutations were performed to assess the significance of the models. Once CNVs were loaded against the pRDA axes, candidates for an association with temperature were determined as those exhibiting a loading greater than 2.25 standard deviations from the mean loading (P < 0.025).

Next, we ran linear mixed models (LMMs) with restricted maximum likelihood optimization where the log-transformed normalized read depth was incorporated as the response variable and temperature as the explanatory variable. The sequencing batch effect was included as a random effect (i.e., random intercepts) to account for the non-independency of observations across batches. One model was performed for each putative CNV, and we used likelihood ratio tests and a FDR of 0.01 following the method of Benjamini & Hochberg (1995) to assess the significance of CNV-temperature associations. We retained the outliers that were detected by both LMMs and pRDA to reduce the number of false positives and represented the overlap with a Venn diagram.

For the 20 strongest CNV loci putatively associated with temperature (those with highest R²), we examined whether discrete copy number categories could be drawn from the distributions of normalized read depth using a model-based unsupervised clustering approach implemented in the R library Mclust, V. 5.4.4 (Fraley et al. 2012). Mclust uses finite mixture estimation via iterative expectation maximization steps (EM) for a range of k components and the best model is selected using the Bayesian Information Criterion (BIC). For each locus, individuals were classified in discrete clusters of normalized read depth (that we coined copy number groups) that likely reflect variation in copy number of any given locus.

Results

Demographic analyses

Influence of temperature on life history and senescence

From 20,033 individual frogs captured 33,857 times at eight study areas (see **Supplementary material S1**, **Tables S1**), we found that life history traits of *R. luteiventris* were strongly associated with mean annual temperature experienced by populations whereas mean annual precipitation showed only a marginal correlation (**Table 1**). Aging rate ranged from 0.11 to 1.51 and increased with increasing temperature (**Table 1**, **Fig.2A**; see **Supplementary material S1**, **Tables S3-S10**). By contrast, lifespan 80% varied between 3.34 and 10.66 years and decreased with increasing temperature (**Table 1**, **Fig.2B**). Similarly, adult survival ranged from 0.26 and 0.78 and was negatively correlated to temperature (**Table 1**, **Fig.2C**). The increase in adult mortality was compensated by higher recruitment (1-seniority) in populations experiencing warm conditions: seniority ranged from 0.26 and 0.94 and was negatively associated with increasing temperature (**Table 1**, **Fig.2D**). Although 95% credible intervals were broad, mean population growth was higher than 1 in 7 of the 8 populations, indicating that almost all populations (except POCR) were likely viable in the long-term (**Supplementary material S1**, **Table S11**). Mean population growth, which varied between 0.77 and 1.13, was not associated with mean annual temperature (**Table 1**). Furthermore, the annual variability of temperature and precipitation showed no significant association with the temporal variance of survival, seniority, and population growth rate (**Table 1**). All demographic estimates from Pradel's models are provided in **Supplementary material S1**, **Table S11.**

Molecular analyses

SNP and CNV discovery

RAD-seq produced 7,095,898 reads per sample on average (range: 1,428,670-10,553,796) before any quality filtering. The mean coverage was 25.56 (range: 8-41). The SNP calling process identified 109,542 SNPs that were successfully genotyped in 352 out of 360 samples initially sequenced (8 samples > 60% missing data were discarded), with a rate of missing data lower than 40% among SNPs. The HDplot approach identified 7,631, 5,787 and 1,523 SNP markers as duplicated, diverged and high coverage respectively (**Supplementary material S1**, **Fig.S2**). All of these markers were distributed over 6,599 putative CNV loci and form the so-called "CNV dataset". Moreover, 13,820 markers were classified as low confidence, and 80,658 markers were classified as singleton SNPs. A total of 29,829 SNPs were pruned during the linkage disequilibrium procedure. The final dataset used in subsequent analyses contained 50,829 SNP singletons, with a global 18.3% missing genotypes.

Putative CNV repeat content

Comparison of the repeat content of putative CNVs relative to the randomly selected sets of RADtags showed that CNVs more commonly fall into LTR elements than expected (OR = 0.65, $p < 0.001$) and consequently, occur less frequently in DNA and MITE elements. Repeat elements containing CNVs were also generally younger (KS test: D = 0.02, p < 0.001; **Supplementary material S1**, **Fig.S8**) although this is seemingly driven by younger DNA elements (**Supplementary material S1**, **Fig.S9-10**). In contrast, LTRs containing CNVs tended to be older than expected (**Supplementary material S1**, **Fig.S9-10**).

Population genetic structure

Using the 50,829 SNPs singletons, we detected very strong population genetic structure. Pairwise F_{ST} calculated between breeding sites were all highly significant and ranged from 0.05 to 0.84, with an average of 0.50 (**Fig.3A**; **Supplementary material S1**, **Table S12**). The Principal Component Analysis revealed a strong genetic differentiation among hydrographic basins (**Fig.3A**).

SNP-temperature associations

SNP-temperature associations revealed a strong signature of thermal adaptation in *R. luteiventris*. The pRDA (**Fig.4A**) designed to detect SNPs associated with temperature was significant ($df = 1$, $F = 17.67$, $p < 0.001$), although the coefficient of determination was low (adjusted $R^2 = 0.045$). A total of 1889 and 234 SNP candidates were associated with temperature based on pRDA and LFMM2, respectively (**Fig.4A**; *p*-values

before and after genomic inflation factor calibration are provided in **Supplementary material S1**, **Fig.S6**). A set of 148 candidate SNPs located on 147 RAD loci were identified by both methods.

Among these 147 RAD loci, BLAST identified 10 loci for which nucleotide sequence had a high similarity with published sequences in other anurans or vertebrates (**Supplementary material S1**, **Table S14)**. BLAST indicated that seven candidate SNPs were located within loci having a high level of similarity with genes regulating resistance to cold and anoxia (locus 155392), gonadotropin-releasing hormone receptor activity (locus 120066), bradykinin production (locus 2796132), organelle biogenesis associated with melanosomes (locus 27203), cell proliferation activity (locus 27781), RNA-binding (locus 2279721), and transcription coactivator activity (locus 117543). Three other loci (2786826, 1770849 and 73386) corresponded to microsatellites described for *R. temporaria*.

CNV-temperature associations

CNV-temperature associations showed strong associations between the normalized read depth of putative CNVs and mean annual temperature. The pRDA (**Fig.4B**) built to detect CNVs associated with temperature was significant ($df = 1$, $F = 9.38$, $p < 0.01$), although the coefficient of determination was low (adjusted $R^2 = 0.023$). The pRDA detected 40 candidate CNVs associated with temperature, whereas LMMs identified 482 candidate CNVs (**Fig.4B**). Here, 39 out of 40 loci detected using the pRDA were also detected by LMMs (**Fig.4B**) and were thus considered as strong candidates. Among the 39 candidate CNVs, 15 CNVs had their normalized read depth positively correlated with temperature while 24 CNVs displayed negative correlations (see **Fig.6** and **Supplementary material S1**, **Table S15**). The sequences of the 39 candidate CNVs had a high similarity with those of DNA repeats identified in the genome of *R. temporaria* (**Supplementary material S1**, **Table S16**). Most candidates (38) were TEs, including 28 TIR transposons of four families (DTA, DTC, DTM, and helitron), one MITE transposon (DTH family), and five LTRs (two of the Gypsy family and three of unknown families).

The identification of discrete groups of copy number categories was examined using the model-based clustering procedure for the 20 strongest CNVs candidates (those with highest R^2 for each category) associated with temperature. This analysis showed that up to three discrete categories can be delineated for candidate CNVs, where each category may represent a specific number of copies for a given locus (**Supplementary material S1**, **Fig.S3** and **S4**).

Discussion

Our analyses showed that *R. luteiventris* life history accelerates with an increase in mean annual temperature: survival was lower, lifespan was shorter, senescence was faster, and recruitment was higher in populations experiencing warmer mean annual temperatures than those exposed to colder conditions. We also found signature of thermal adaptation at the molecular level: we identified SNPs associated with mean annual temperature that were located within the body of protein-coding genes regulating diverse biological processes including cold resistance. Furthermore, we found several CNV candidates (especially transposable elements) whose normalized read depth was associated with temperature, suggesting that thermal conditions may influence copy number variation within the *R. luteiventris* genome.

Temperature-dependent life history variation

Our results indicated that the position of *R. luteiventris* populations along the fast-slow continuum of life history was strongly associated with temperature whereas mean annual precipitation had a marginal effect on demographic parameters. In populations experiencing low mean annual temperature, which typically occurred at higher elevations and latitudes, individuals had higher adult survival, longer lifespan, and lower senescence rate than those from warmer environments. Interestingly, increased adult mortality was compensated by high recruitment in populations experiencing warm conditions. This compensatory recruitment (a mechanism also observed in amphibian response to parasites, see Valenzuela-Sánchez et al. 2021) resulted in positive population growth rate in seven of the eight *R. luteiventris* populations we studied.

The temperature-dependent increase in mortality found using our long-term capture-recapture data are congruent with the results of many skeletochronological studies that have highlighted an increase in median age and maximal longevity with altitude and latitude at the intraspecific level (Zhang & Lu 2012, Sinsch et al. 2015, Zhong et al. 2018). The increase in recruitment with increasing temperature in our study system is also congruent with the reduction of breeding frequency and clutch size (relative to body size) reported in many anuran populations at high altitude and latitude (Morrison & Hero 2003). Overall, our study and previous ones indicate that temperature produces similar effects on anuran life history at intraspecific and interspecific levels (Zhang & Lu 2012, Stark & Meiri 2018), promoting slow strategies under cold conditions and fast strategies in warmer environments.

Our results showed for the first time a positive effect of temperature on senescence rate among wild populations, thus confirming senescence acceleration with temperature observed under laboratory conditions in model organisms of aging (*Drosophila melanogaster*, Jacobson et al. 2010; *Notobranchius furzeri*, Valenzano et al. 2006; *Caenorhabditis elegans*, Yen & Mobbs 2010). We found that senescence rate was 14 times higher

in the population experiencing the warmest conditions (8.35° C) compared to the one with the coldest temperature (1.71° C). Senescence rate varied from 0.11 to 1.51, a broader range of values than what has been reported for female mammals (senescence rate calculated from Siler models: 0.01-1.17) at a broad phylogenetic scale (Lemaître et al. 2020). Overall, our analyses and a previous study on the yellow-bellied toad *Bombina variegata* (Cayuela et al. 2020b) suggest that amphibian senescence patterns can display high intraspecific variation (but see also Cayuela et al. 2019) and may be highly sensitive to environmental variation.

Genomic signatures of thermal adaptation

We identified 148 strong SNP candidates associated with temperature using a conservative approach combining two GEA methods. Despite the large number of SNPs (50,829) and non-duplicated loci (37,499) discovered in our study, the number of SNP candidates potentially involved in thermal adaptation is likely underestimated since we used a reduced representation method (Lowry et al. 2017) in an amphibian with a large genome size (~9 Gbp in the Oregon spotted frog *Rana pretiosa*, a sister species of *R. luteiventris*, http://www.genomesize.com/). Among the 148 SNP candidates, BLAST identified 10 loci for which nucleotide sequence displayed a high similarity with published sequences in other anurans. This limited number of BLAST hits probably resulted from the absence of annotated reference genome for anurans phylogenetically related to *R. luteiventris*.

We identified three candidate SNPs located within the body of protein-coding genes that could play a critical role in thermal adaptation and might be involved in temperature-dependent life history variation. One SNP could especially contribute to the recruitment changes detected in our study. This marker was located within a locus having a high sequence similarity with the gene GnRH receptor-3 that regulates gonadotropin-releasing hormone receptor activity in another Nearctic anuran, the American bullfrog *Lithobates catesbeianus*. This gonadotropin-releasing hormone is a peptide hormone responsible for the release of follicle-stimulating hormone (FSH) and luteinizing hormone (LH) from the anterior pituitary in vertebrates (Norris & Carr 2020). In amphibians, FSH and LH regulate hormone steroid secretion (progesterone, 17β-estradiol, testosterone, and 5a-dihydrotestosterone), gametogenesis, and mating behavior (Moore 1987, Aranzábal 2011, Propper 2011). Mutations on this gene could modulate breeding effort in both sexes along the temperature gradient and might be involved in the temperature-related life history patterns highlighted in our demographic analyses.

Two candidate SNPs were also located within the body of genes that regulate resistance to cold and hypoxia in anurans and might contribute to the extended lifespan and the slow senescence observed in *R. luteiventris* populations experiencing low mean annual temperature. One of the two SNP candidates was

positioned on a locus which had high sequence similarity to the gene *Aat* (Matsuba et al. 2007), which codes for ADP/ATP translocase (AAT), an enzyme involved in freeze and hypoxia resistance in the wood frog, *Lithobates sylvaticus* (Cai et al. 1997). The other SNP candidate was located within the body of the bradykinin precursor gene that regulates bradykinin production. This gene may be directly involved in adaptation to cold since bradykinin-like peptides secreted from amphibian skin may act to increase microvascular permeability (Xi et al. 2015). This physiological response could facilitate skin respiration (Tattersall 2007) and limit mortality due to hypoxia in cold-adapted populations experiencing long periods of aquatic overwintering, such as *R. luteiventris* (Bull & Hayes 2002, Tattersall & Ultsch 2008).

The bradykinin precursor gene could also regulate immune response to pathogen-climate interactions in *R. luteiventris*. Bradykinin is one of the most abundant (and well studied, see Xi et al. 2015) antimicrobial peptides in ranid skin secretion that inhibit the growth of the pathogenic chytrid fungus (*Batrachochytrium dendrobatidis*, *Bd*) (Rollins-Smith et al. 2006) causing chytridiomycosis. *Bd* is broadly spread across the western USA and can have high prevalence level in *R. luteiventris* populations (Pearl et al. 2007, Adams et al. 2010, Russell et al. 2010). *Bd* prevalence increases with elevation in ranid populations of this region (Pearl et al. 2009, Piovia-Scott et al. 2011), leading to higher infection risk in cold environments where anurans are less likely to clear *Bd* infections by increasing their body temperature (Woodhams et al. 2003, Richards-Zawacki 2010, Russell et al. 2010). Research indicates that antimicrobial peptides inhibit *Bd* (in bioassays) in *R. luteiventris*, although inhibition is not necessarily correlated with *Bd* intensity in frogs (Loudon et al. 2020). We propose that mutations in the bradykinin precursor gene could play a role in temperature-mediated evolutionary response to *Bd* in *R. luteiventris*. Further studies could investigate how this sequence polymorphism may influence bradykinin secretion and modulate the evolution of tolerance and resistance to *Bd* in cold-adapted populations.

Although the candidate SNPs detected by the GEA are likely hitchhiking markers rather than causal variants, our results suggest that sequence polymorphisms on several candidate genes regulating reproductive activity, immunity, and resistance to cold and hypoxia/anoxia could eventually be found to contribute to thermal adaptation in *R. luteiventris*. This SNP-based signal is congruent with the findings of three previous studies that have highlighted molecular signatures of thermal adaptation in ranid and bufonid species from Europe (Common frog *R. temporaria*, Rödin-Mörch et al. 2019; Common toad *Bufo bufo* Rödin-Mörch et al. 2021) and Asia (Yang et al. 2016). In particular, a comparative transcriptome study (Yang et al. 2016) focused on three anuran species (Asiatic toad *Bufo gargarizans*, Plateau brown frog *Rana kukunoris*, and Asiatic grass frog *Rana chensinensis*) from the Tibetan region found that altitude determined allele frequency of large set of genes notably regulating immune response, metabolism, and longevity. Interestingly, skeletochronological data

revealed that maximal longevity and/or median age increased with altitude or latitude in several of these species (*R. temporaria*, Hjernquist et al. 2012; *B. gargarizans*, Yu & Lu 2013; *R. chensinensis*, Ma et al. 2009).

Our study adds to a growing body of work suggesting that temperature-dependent life history acceleration commonly observed in anurans could be partially regulated by SNPs evolving under polygenic selection. However, the functional links between this life history variation and the candidate SNPs detected by GEA still remain to be deciphered using whole-genome and transcriptome sequencing data. Novel GWAS (Genome-Wide Association Studies) approaches based on capture-recapture modeling, where genotype-survival and genotype-senescence associations can control for imperfect detection probability, still need to be developed to tackle this issue in wild animal populations.

Temperature-dependent accumulation of transposable elements

Our study also highlighted CNV–temperature associations: a total of 39 candidate CNVs were detected using a conservative approach combining regression and redundancy analyses. The normalized read depth of 24 and 15 duplicated regions were negatively and positively correlated with temperature, respectively. Thirty-eight candidates were TEs, and 63% (24) were transposons that have diverged more recently than the other elements of their own family. Overall, these results suggest that relatively recent temperature changes determined TE accumulation patterns within *R. luteiventris* genome.

Although these mechanisms are still poorly understood in amphibians, temperature-dependent TE accumulations have been recently documented in fishes (Carducci et al. 2020, Cayuela et al. 2021). A study on a marine fish using similar RAD-seq CNV analyses found associations between the normalized read depth of transposons and retrotransposons and water temperature (Cayuela et al. 2021). Furthermore, phylogenetic analysis performed on 39 teleost species highlighted an unexpected clusterization of a non-LTR retrotransposon isolated from species living in cold waters compared with those isolated from species living in warmer waters (Carducci et al. 2019). In *R. luteiventris*, temperature-dependent accumulations of recently diverged TEs likely result from thermal stresses endured during individual lifetime, as proposed in fishes (Carducci et al. 2020). This TE accumulation, potentially caused by thermo-induced epigenetic changes (Rey et al. 2016), could be involved in the temperature-dependent changes in senescence and lifespan observed in *R. luteiventris* since studies showed that activation of TE expression leads to an acceleration of cell aging through inflammatory pathways (Andrenacci et al. 2020) and is partially responsible of sex-related differences in longevity and aging (Brown et al. 2020).

Conclusions

Our study highlighted that, in ectotherms like *R. luteiventris*, variation in thermal conditions leads to important clinal changes in life history, notably including an acceleration in senescence with increasing temperature. We also detected molecular signatures of thermal adaptation involving candidate genes that might play a role in this life history shift. In addition, temperature-dependent accumulation of recently diverged transposons and retrotransposons in *R. luteiventris* genome might also have an impact on life history traits including senescence. Further studies based on whole-genome sequencing data and novel GWAS approaches controlling for recapture probability will help clarify functional links between SNPs, CNVs (especially TEs) and individual mortality metrics across populations experiencing contrasting thermal conditions. A better understanding of these mechanisms will be crucial to understanding and predicting the impact of climate change on ectotherm populations.

Data availability statement

Genomic data are available on Dryad (https://doi.org/10.5061/dryad.x3ffbg7k3).

Author contributions

H.C. completed the demographic analyses and wrote the paper. B.R.F, D.L.J., and Y.D. contributed to the bioinformatics and genomic analyses. B.R.F., D.S.P., H.C., R.M.M., and W.C.F. initiated and conceptualized the project. H.C. coordinated the work. D.S.P., L.E, B.H., and R.M.M. collected demographic and DNA samples. J.M.W.G. conceived the maps and extracted environmental data. All authors read and edited the final manuscript version.

References

Adams, M. J., Chelgren, N. D., Reinitz, D., Cole, R. A., Rachowicz, L. J., Galvan, S., McCreary, B., Pearl, C. A., Bailey, L. L., Bettaso, J., Bull, E. L., & Leu, M. (2010). Using occupancy models to understand the distribution of an amphibian pathogen, *Batrachochytrium dendrobatidis*. Ecological Applications, 20, 289-302.

Amish, S. J., Ali, O., Peacock, M., Miller, M., Robinson, M., Smith, S., Luikart, G., & Neville, H. (2019). Assessing thermal adaptation using family-based association and FST outlier tests in a threatened trout species. Molecular ecology, 28, 2573-2593.

Andrenacci, D., Cavaliere, V., & Lattanzi, G. (2020). The role of transposable elements activity in aging and their possible involvement in laminopathic diseases. Ageing research reviews, 57, 100995.

Andrews, S. (2019). FastQC: a quality control tool for high throughput sequence data (Version 0.11.8). Retrieved from http://www.bioinformatics.babraham.ac.uk/projects/fastqc/

Angilletta, M. J., Steury, T. D., & Sears, M. W. (2004). Temperature, growth rate, and body size in ectotherms: fitting pieces of a life-history puzzle. Integrative and comparative biology, 44, 498-509.

Aranzábal, M. C. U. (2011). Hormones and the female reproductive system of amphibians. In Hormones and reproduction of vertebrates (pp. 55-81). Academic Press.

Benestan, L., Quinn, B. K., Maaroufi, H., Laporte, M., Clark, F. K., Greenwood, S. J., Rochette, R., & Bernatchez, L. (2016). Seascape genomics provides evidence for thermal adaptation and current-mediated population structure in American lobster (*Homarus americanus*). Molecular Ecology, 25, 5073-5092.

Benjamini, Y., & Hochberg, Y. (1995). Controlling the false discovery rate: a practical and powerful approach to multiple testing. Journal of the Royal statistical society: series B (Methodological), 57, 289-300.

Blanck, A., & Lamouroux, N. (2007). Large-scale intraspecific variation in life-history traits of European freshwater fish. Journal of Biogeography, 34, 862-875.

Bodensteiner, B. L., Agudelo-Cantero, G. A., Arietta, A. A., Gunderson, A. R., Muñoz, M. M., Refsnider, J. M., & Gangloff, E. J. (2021). Thermal adaptation revisited: How conserved are thermal traits of reptiles and amphibians?. Journal of Experimental Zoology Part A: Ecological and Integrative Physiology, 335, 173-194.

Bourque, G., Burns, K. H., Gehring, M., Gorbunova, V., Seluanov, A., Hammell, M., Imbeault, M., Izsvák, Z., Levin, H. L., Macfarlan, T. S., Mager, D. L., & Feschotte, C. (2018). Ten things you should know about transposable elements. Genome Biology, 19, 1-12.

Brown, E. J., Nguyen, A. H., & Bachtrog, D. (2020). The Y chromosome may contribute to sex-specific ageing in Drosophila. Nature ecology & evolution, 4, 853-862.

Bull, E. L., & Hayes, M. P. (2002). Overwintering of Columbia spotted frogs in Northeastern Oregon. Northwest Science, 76, 141-147.

Burraco, P., Orizaola, G., Monaghan, P., & Metcalfe, N. B. (2020). Climate change and ageing in ectotherms. Global Change Biology, 26, 5371-5381.

Cai, Q., Greenway, S. C., & Storey, K. B. (1997). Differential regulation of the mitochondrial ADP/ATP translocase gene in wood frogs under freezing stress. Biochimica et Biophysica Acta (BBA)-Gene Structure and Expression, 1353, 69-78.

Catchen, JM, Amores, A., Hohenlohe, P., Cresko, W., & Postlethwait, J. (2011). Stacks: Building and genotyping loci de novo from short-read sequences. G3 Genes Genomes Genetics, 1, 171–182.

Catchen, Julian, Hohenlohe, P. A., Bassham, S., Amores, A., & Cresko, W. A. (2013). Stacks: An analysis tool set for population genomics. Molecular Ecology, 22, 3124–3140.

Caye, K., Jumentier, B., Lepeule, J., & François, O. (2019). LFMM 2: fast and accurate inference of gene-environment associations in genome-wide studies. Molecular Biology and Evolution, 36, 852-860.

Campbell-Staton, S. C., Winchell, K. M., Rochette, N. C., Fredette, J., Maayan, I., Schweizer, R. M., & Catchen, J. (2020). Parallel selection on thermal physiology facilitates repeated adaptation of city lizards to urban heat islands. Nature Ecology & Evolution, 4, 652-658.

Carducci, F., Biscotti, M. A., Forconi, M., Barucca, M., & Canapa, A. (2019). An intriguing relationship between teleost Rex3 retroelement and environmental temperature. Biology Letters, 15, 20190279.

Carducci, F., Barucca, M., Canapa, A., Carotti, E., & Biscotti, M. A. (2020). Mobile elements in ray-finned fish genomes. Life, 10, 221.

Casacuberta, E., & González, J. (2013). The impact of transposable elements in environmental adaptation. Molecular ecology, 22(6), 1503-1517.

Cayuela, H., Olgun, K., Angelini, C., Üzüm, N., Peyronel, O., Miaud, C., Avcı, A., Lemaitre, J.-F., & Schmidt, B. R. (2019). Slow life-history strategies are associated with negligible actuarial senescence in western Palaearctic salamanders. Proceedings of the Royal Society B, 286, 20191498.

Cayuela, H., Rougemont, Q., Laporte, M., Mérot, C., Normandeau, E., Dorant, Y., Tørresen, O. K., Hoff, S. N. K., Jentoft, S., Sirois, P., Castonguay, M., Jansen, T., Praebel, K., Clément, M., & Bernatchez, L. (2020a). Shared ancestral polymorphisms and chromosomal rearrangements as potential drivers of local adaptation in a marine fish. Molecular Ecology, 29, 2379-2398.

Cayuela, H., Lemaître, J. F., Bonnaire, E., Pichenot, J., & Schmidt, B. R. (2020b). Population position along the fast–slow life-history continuum predicts intraspecific variation in actuarial senescence. Journal of Animal Ecology, 89, 1069-1079.

Cayuela, H., Dorant, Y., Mérot, C., Laporte, M., Normandeau, E., Gagnon-Harvey, S., Clément, M. Sirois, P., & Bernatchez, L. (2021). Thermal adaptation rather than demographic history drives genetic structure inferred by copy number variants in a marine fish. Molecular Ecology, 30, 1624-1641.

Chang, C. C., Chow, C. C., Tellier, L. C., Vattikuti, S., Purcell, S. M., & Lee, J. J. (2015). Second-generation PLINK: Rising to the challenge of larger and richer datasets. GigaScience, 4.

Chen, Z., Cheng, C. H. C., Zhang, J., Cao, L., Chen, L., Zhou, L., Jin, Y., Ye, H., Deng, C., Dai, Z., Xu, Q., Hu, P., Sun, S., Shen, Y, & Chen, L. (2008). Transcriptomic and genomic evolution under constant cold in Antarctic notothenioid fish. Proceedings of the National Academy of Sciences, 105, 12944-12949.

Chen, Z., & Narum, S. R. (2021). Whole genome resequencing reveals genomic regions associated with thermal adaptation in redband trout. Molecular Ecology, 30, 162-174.

Chuong, E. B., Elde, N. C., & Feschotte, C. (2017). Regulatory activities of transposable elements: from conflicts to benefits. Nature Reviews Genetics, 18, 71.

Colchero, F., & Clark, J. S. (2012). Bayesian inference on age-specific survival for censored and truncated data. Journal of Animal Ecology, 81, 139-149.

Colchero, F., Jones, O. R., & Rebke, M. (2012). BaSTA: an R package for Bayesian estimation of age-specific survival from incomplete mark–recapture/recovery data with covariates. Methods in Ecology and Evolution, 3, 466-470.

Colombo, A. R., Elias, H. K., & Ramsingh, G. (2018). Senescence induction universally activates transposable element expression. Cell Cycle, 17, 1846-1857.

Dorant, Y., Cayuela, H., Wellband, K., Laporte, M., Rougemont, Q., Mérot, C., Normandeau, E., Rochette, R., & Bernatchez, L. (2020). Copy number variants outperform SNPs to reveal genotype–temperature association in a marine species. Molecular Ecology, 29, 4765-4782.

Flouris, A. D., & Piantoni, C. (2015). Links between thermoregulation and aging in endotherms and ectotherms. Temperature, 2, 73-85.

Forester, B. R., Lasky, J. R., Wagner, H. H., & Urban, D. L. (2018). Comparing methods for detecting multilocus adaptation with multivariate genotype–environment associations. Molecular Ecology, 27, 2215-2233.

Fraley, C., Raftery, A. E., Murphy, T. B., & Scrucca, L. (2012). mclust version 4 for R: normal mixture modeling for model-based clustering, classification, and density estimation (Vol. 597, p. 1). Technical report.

François, O., Martins, H., Caye, K., & Schoville, S. D. (2016). Controlling false discoveries in genome scans for selection. Molecular ecology, 25, 454-469.

Frichot, E., Schoville, S. D., Bouchard, G., & François, O. (2013). Testing for associations between loci and environmental gradients using latent factor mixed models. Molecular Biology and Evolution, 30, 1687-1699.

Frichot, E., & François, O. (2015). LEA: An R package for landscape and ecological association studies. Methods in Ecology and Evolution, 6, 925-929.

Gugger, P. F., Liang, C. T., Sork, V. L., Hodgkiss, P., & Wright, J. W. (2018). Applying landscape genomic tools to forest management and restoration of Hawaiian koa (*Acacia ko*a) in a changing environment. Evolutionary Applications, 11, 231–242.

Gunderson, A. R., & Stillman, J. H. (2015). Plasticity in thermal tolerance has limited potential to buffer ectotherms from global warming. Proceedings of the Royal Society B: Biological Sciences, 282, 20150401.

Hjernquist, M. B., Söderman, F., Jönsson, K. I., Herczeg, G., Laurila, A., & Merilä, J. (2012). Seasonality determines patterns of growth and age structure over a geographic gradient in an ectothermic vertebrate. Oecologia, 170, 641-649.

Huey, R. B., & Berrigan, D. (2001). Temperature, demography, and ectotherm fitness. The American Naturalist, 158, 204-210.

IPCC (2014). IPCC Climate Change 2014: Synthesis Report. Contribution of Working Groups I, II and III to the Fifth Assessment Report of the Intergovernmental Panel on Climate Change, IPCC, Geneva, Switzerland (2014), p. 151

Jacobson, J., Lambert, A. J., Portero-Otín, M., Pamplona, R., Magwere, T., Miwa, S., Driege, Y., Brand, M. D, & Partridge, L. (2010). Biomarkers of aging in Drosophila. Aging Cell, 9, 466-477.

Keil, G., Cummings, E., & de Magalhaes, J. P. (2015). Being cool: how body temperature influences ageing and longevity. Biogerontology, 16, 383-397.

Krueger, F. (2019). Trim Galore! (Version 0.6.4). http://www.bioinformatics.babraham.ac.uk/projects/trim_galore/

Legendre, P., & Legendre, L. (2012). Numerical ecology. Elsevier.

Lemaître, J. F., Ronget, V., Tidière, M., Allainé, D., Berger, V., Cohas, A., Colchero, F., Conde, D. A., Garratt, M., Liker, A., Marais, G. A. B., Scheuerlein, A. Székely, T., & Gaillard, J.M. (2020). Sex differences in adult lifespan and aging rates of mortality across wild mammals. Proceedings of the National Academy of Sciences, 117, 8546-8553.

Lehnert, S. J., DiBacco, C., Van Wyngaarden, M., Jeffery, N. W., Lowen, J. B., Sylvester, E. V., ... & Bradbury, I. R. (2019). Fine-scale temperature-associated genetic structure between inshore and offshore populations of sea scallop (*Placopecten magellanicus*). Heredity, 122, 69-80.

Loudon, A. H., Kurtz, A., Esposito, E., Umile, T. P., Minbiole, K. P. C., Parfrey, L. W., & Sheafor, B. A. (2020). Columbia spotted frogs (*Rana luteiventris*) have characteristic skin microbiota that may be shaped by cutaneous skin peptides and the environment. FEMS Microbiology Ecology, 96, fiaa168.

Lowry, D. B., Hoban, S., Kelley, J. L., Lotterhos, K. E., Reed, L. K., Antolin, M. F., & Storfer, A. (2017). Breaking RAD: An evaluation of the utility of restriction site-associated DNA sequencing for genome scans of adaptation. Molecular Ecology, 17, 141-152.

Ma, X., Tong, L., & Lu, X. (2009). Variation of body size, age structure and growth of a temperate frog, *Rana chensinensis*, over an elevational gradient in northern China. Amphibia-Reptilia, 30, 111-117.

Mallard, F., Nolte, V., Tobler, R., Kapun, M., & Schlötterer, C. (2018). A simple genetic basis of adaptation to a novel thermal environment results in complex metabolic rewiring in Drosophila. Genome Biology, 19, 1-15.

Martin, M. (2011). Cutadapt removes adapter sequences from high-throughput sequencing reads. EMBnet.Journal, 17, 10–12.

Matsuba, C., Uolevi Palo, J., Kuzmin, S. L., & Merilä, J. (2007). Evidence for multiple retroposition events and gene evolution in the ADP/ATP translocase gene family in Ranid frogs. Journal of Heredity, 98, 300-310.

Mérot, C., Oomen, R. A., Tigano, A., & Wellenreuther, M. (2020). A roadmap for understanding the evolutionary significance of structural genomic variation. Trends in Ecology & Evolution, 35, 561-572.

Mims, M. C., Olson, D. H., Pilliod, D. S., & Dunham, J. B. (2018). Functional and geographic components of risk for climate sensitive vertebrates in the Pacific Northwest, USA. Biological Conservation, 228, 183-194

Moore, F. L. (1987). Reproductive endocrinology of amphibians. In Fundamentals of comparative vertebrate endocrinology (pp. 207-221). Springer, Boston, MA.

Morrison, C., & Hero, J. M. (2003). Geographic variation in life-history characteristics of amphibians: a review. Journal of Animal Ecology, 72, 270-279.

Munch, S. B., & Salinas, S. (2009). Latitudinal variation in lifespan within species is explained by the metabolic theory of ecology. Proceedings of the National Academy of Sciences, 106, 13860-13864.

Norris, D. O., & Carr, J. A. (2020). Vertebrate endocrinology. Academic Press.

Paris, J. R., Stevens, J. R., & Catchen, J. M. (2017). Lost in parameter space: A road map for stacks. Methods in Ecology and Evolution, 8, 1360–1373.

Parker, D. J., Wiberg, R. A. W., Trivedi, U., Tyukmaeva, V. I., Gharbi, K., Butlin, R. K., Hoikkala, A., Kankare, & Ritchie, M. G. (2018). Inter and intraspecific genomic divergence in *Drosophila montana* shows evidence for cold adaptation. Genome Biology and Evolution, 10, 2086-2101.

Pearl, C. A., Bull, E. L., Green, D. E., Bowerman, J., Adams, M. J., Hyatt, A., & Wente, W. H. (2007). Occurrence of the amphibian pathogen *Batrachochytrium dendrobatidis* in the Pacific Northwest. Journal of Herpetology, 41, 145-149.

Pearl, C. A., Bowerman, J., Adams, M. J., & Chelgren, N. D. (2009). Widespread occurrence of the chytrid fungus *Batrachochytrium dendrobatidis* on Oregon spotted frogs (*Rana pretiosa*). EcoHealth, 6, 209-218.

Pembleton, L. W., Cogan, N. O. I., & Forster, J. W. (2013). StAMPP: An R package for calculation of genetic differentiation and structure of mixed-ploidy level populations. Molecular Ecology Resources, 13, 946–952.

Perrier, C., Ferchaud, A. L., Sirois, P., Thibault, I., & Bernatchez, L. (2017). Do genetic drift and accumulation of deleterious mutations preclude adaptation? Empirical investigation using RAD seq in a northern lacustrine fish. Molecular Ecology, 26, 6317-6335.

Peterson, B. K., Weber, J. N., Kay, E. H., Fisher, H. S., & Hoekstra, H. E. (2012). Double digest RADseq: An inexpensive method for de novo SNP discovery and genotyping in model and non-model species. PLoS ONE, 7, e37135.

Pilliod, D. S., Arkle, R. S., Robertson, J. M., Murphy, M. A., & Funk, W. C. (2015). Effects of changing climate on aquatic habitat and connectivity for remnant populations of a wide-ranging frog species in an arid landscape. Ecology and Evolution, 5, 3979-3994.

Pilliod, D. S., Hausner, M. B., & Scherer, R. D. (2021). From satellites to frogs: Quantifying ecohydrological change, drought mitigation, and population demography in desert meadows. Science of The Total Environment, 758, 143632.

Piovia-Scott, J., Pope, K. L., Lawler, S. P., Cole, E. M., & Foley, J. E. (2011). Factors related to the distribution and prevalence of the fungal pathogen *Batrachochytrium dendrobatidis* in *Rana cascadae* and other amphibians in the Klamath Mountains. Biological Conservation, 144(12), 2913-2921.

Plummer, M. (2003). JAGS: A program for analysis of Bayesian graphical models using Gibbs sampling. In Proceedings of the 3rd international workshop on distributed statistical computing (Vol. 124, No. 125.10, pp. 1-10).

Plummer, M., Best, N., Cowles, K., Vines, K., Sarkar, D., & Almond, R. (2006). CODA: Output analysis and diagnostics for MCMC. 0.16. URL https://CRAN. R-project. org/package= coda. R package version 0.19-3.

Promislow, D. E., & Harvey, P. H. (1990). Living fast and dying young: A comparative analysis of life-history variation among mammals. Journal of Zoology, 220, 417-437.

Propper, C. R. (2011). Testicular structure and control of sperm development in amphibians. In Hormones and Reproduction of Vertebrates (pp. 39-53). Academic Press.

Quigley, K. M., Bay, L. K., & van Oppen, M. J. (2020). Genome-wide SNP analysis reveals an increase in adaptive genetic variation through selective breeding of coral. Molecular Ecology, 29, 2176-2188.

R Core Team (2019). R: A language and environment for statistical computing. R Foundation for Statistical Computing, Vienna, Austria. URL http://www.R-project.org/.

Rajpurohit, S., Gefen, E., Bergland, A. O., Petrov, D. A., Gibbs, A. G., & Schmidt, P. S. (2018). Spatiotemporal dynamics and genome-wide association analysis of desiccation tolerance in Drosophila melanogaster. Molecular Ecology, 27, 3525-3540.

Rey, O., Danchin, E., Mirouze, M., Loot, C., & Blanchet, S. (2016). Adaptation to global change: a transposable element–epigenetics perspective. Trends in Ecology & Evolution, 31, 514-526.

Richards-Zawacki, C. L. (2010). Thermoregulatory behaviour affects prevalence of chytrid fungal infection in a wild population of Panamanian golden frogs. Proceedings of the Royal Society B: Biological Sciences, 277, 519-528.

Rochette, N. C., Rivera-Colón, A. G., & Catchen, J. M. (2019). Stacks 2: Analytical methods for paired-end sequencing improve RADseq-based population genomics. Molecular Ecology, 28, 4737–4754.

Rödin-Mörch, P., Luquet, E., Meyer-Lucht, Y., Richter-Boix, A., Höglund, J., & Laurila, A. (2019). Latitudinal divergence in a widespread amphibian: Contrasting patterns of neutral and adaptive genomic variation. Molecular Ecology, 28, 2996-3011.

Rödin-Mörch, P., Palejowski, H., Cortazar-Chinarro, M., Kärvemo, S., Richter-Boix, A., Höglund, J., & Laurila, A. (2021). Small-scale population divergence is driven by local larval environment in a temperate amphibian. Heredity, 126, 279-292.

Rodríguez, A., Rusciano, T., Hamilton, R., Holmes, L., Jordan, D., & Wollenberg Valero, K. C. (2017). Genomic and phenotypic signatures of climate adaptation in an Anolis lizard. Ecology and Evolution, 7, 6390-6403.

Rollins-Smith, L. A., Woodhams, D. C., Reinert, L. K., Vredenburg, V. T., Briggs, C. J., Nielsen, P. F., & Conlon, J. M. (2006). Antimicrobial peptide defenses of the mountain yellow-legged frog (*Rana muscosa*). Developmental & Comparative Immunology, 30, 831-842.

Ronget, V., & Gaillard, J. M. (2020). Assessing ageing patterns for comparative analyses of mortality curves: Going beyond the use of maximum longevity. Functional Ecology, 34, 65-75.

Russell, D. M., Goldberg, C. S., Waits, L. P., & Rosenblum, E. B. (2010). *Batrachochytrium dendrobatidis* infection dynamics in the Columbia spotted frog *Rana luteiventris* in north Idaho, USA. Diseases of Aquatic Organisms, 92, 223-230.

Schweyen, H., Rozenberg, A., & Leese, F. (2014). Detection and Removal of PCR Duplicates in Population Genomic ddRAD Studies by Addition of a Degenerate Base Region (DBR) in Sequencing Adapters. The Biological Bulletin, 227, 146–160.

Seebacher, F., White, C. R., & Franklin, C. E. (2015). Physiological plasticity increases resilience of ectothermic animals to climate change. Nature Climate Change, 5, 61-66.

Selwood, K. E., McGeoch, M. A., & Mac Nally, R. (2015). The effects of climate change and land-use change on demographic rates and population viability. Biological Reviews, 90, 837-853.

Siler, W. (1979). A competing-risk model for animal mortality. Ecology, 60, 750-757.

Sinsch, U. (2015). Skeletochronological assessment of demographic life-history traits in amphibians. The Herpetological Journal, 25, 5-13.

Smit, A. F. A, Hubley, R. & Green, P. (2015) RepeatMasker Open-4.0, http://www.repeatmasker.org

Stark, G., & Meiri, S. (2018). Cold and dark captivity: drivers of amphibian longevity. Global Ecology and Biogeography, 27, 1384-1397.

Stenseth, N. C., & Mysterud, A. (2002). Climate, changing phenology, and other life history traits: nonlinearity and match–mismatch to the environment. Proceedings of the National Academy of Sciences, 99, 13379-13381.

Su, Y. S., & Yajima, M. (2012). R2jags: A Package for Running jags from R. R package version 0.03-08, URL http://CRAN. R-project. org/package= R2jags.

Tattersall, G. (2007). Skin breathing in amphibians. Endothelial Biomedicine: a Comprehensive Reference, 85-91

Tattersall, G. J., & Ultsch, G. R. (2008). Physiological ecology of aquatic overwintering in ranid frogs. Biological Reviews, 83, 119-140.

Tenan, S., Pradel, R., Tavecchia, G., Igual, J. M., Sanz-Aguilar, A., Genovart, M., & Oro, D. (2014). Hierarchical modelling of population growth rate from individual capture–recapture data. Methods in Ecology and Evolution, 5, 606-614.

Valenzano, D. R., Terzibasi, E., Cattaneo, A., Domenici, L., & Cellerino, A. (2006). Temperature affects longevity and age-related locomotor and cognitive decay in the short-lived fish Nothobranchius furzeri. Aging Cell, 5, 275-278.

Valenzuela-Sánchez, A., Wilber, M. Q., Canessa, S., Bacigalupe, L. D., Muths, E., Schmidt, B. R., Cunningham, A. A., Ozgul, A., Johnson, P. T. J., & Cayuela, H. (2021). Why disease ecology needs life-history theory: a host perspective. Ecology Letters, 24, 876-890.

Walsh, B. S., Parratt, S. R., Hoffmann, A. A., Atkinson, D., Snook, R. R., Bretman, A., & Price, T. A. (2019). The impact of climate change on fertility. Trends in Ecology & Evolution, 34, 249-259.

Wei, S., Li, Z., Momigliano, P., Fu, C., Wu, H., & Merilä, J. (2020). The roles of climate, geography and natural selection as drivers of genetic and phenotypic differentiation in a widespread amphibian Hyla annectans (Anura: Hylidae). Molecular Ecology, 29, 3667-3683.

Wellenreuther, M., Mérot, C., Berdan, E., & Bernatchez, L. (2019). Going beyond SNPs: The role of structural genomic variants in adaptive evolution and species diversification. Molecular Ecology, 28, 1203-1209.

Woodhams, D. C., Alford, R. A., & Marantelli, G. (2003). Emerging disease of amphibians cured by elevated body temperature. Diseases of aquatic organisms, 55, 65-67.

Xi, X., Li, B., Chen, T., & Kwok, H. F. (2015). A review on bradykinin-related peptides isolated from amphibian skin secretion. Toxins, 7, 951-970.

Yen, K., & Mobbs, C. V. (2010). Evidence for only two independent pathways for decreasing senescence in Caenorhabditis elegans. Age, 32, 39-49.

Yu, T., & Lu, X. (2013). Body size variation of four latitudinally-separated populations of a toad species: age and growth rate as the proximate determinants. Integrative Zoology, 8, 315-323.

Yang, W., Qi, Y., & Fu, J. (2016). Genetic signals of high-altitude adaptation in amphibians: a comparative transcriptome analysis. BMC genetics, 17, 1-10.

Zhang, L., & Lu, X. I. N. (2012). Amphibians live longer at higher altitudes but not at higher latitudes. Biological Journal of the Linnean Society, 106, 623-632.

Zhong, M., Yu, X., & Liao, W. (2018). A review for life-history traits variation in frogs especially for anurans in China. Asian Herpetological Research, 9, 165-174.

Table 1. Effect of temperature and precipitation on demographic parameters in eight populations of *R. luteiventris*. Likelihood ratio tests were used to assess the influence of mean and temporal variance (SD) of temperature (calculated for the period 1990-2019) and precipitation on aging rate, lifespan 80%, annual adult survival (mean μ and temporal variance σ), annual seniority (μ and σ), and annual population growth rate (μ and σ). Recruitment is approximated as 1-seniority. R² values were calculated from the linear model. Relationships for which likelihood ratio test had a p-value lower than 0.05 are shown in bold.

| Parameter	*df*	χ^2	p-value	R^2
Mean annual temperature				
Aging rate	1	**10.13**	**0.001**	**0.73**
Lifespan 80%	1	**5.32**	**0.02**	**0.49**
Survival (μ)	1	**8.18**	**0.004**	**0.60**
Seniority (μ)	1	**7.69**	**0.005**	**0.58**
Population growth (μ)	1	0.17	0.68	0.02
Mean annual cumulative precipitation				
Aging rate	1	3.05	0.08	0.31
Lifespan 80%	1	0.88	0.35	0.10
Survival (μ)	1	2.15	0.14	0.21
Seniority (μ)	1	2.14	0.14	0.21
Population growth (μ)	1	0.15	0.69	0.02
Standard deviation of annual temperature				
Survival (σ)	1	0.008	0.93	0.05
Seniority (σ)	1	0.31	0.57	0.03
Population growth (σ)	1	0.26	0.61	0.03
Standard deviation of n annual cumulative precipitation				
Survival (σ)	1	0.47	0.49	0.05
Seniority (σ)	1	0.05	0.82	0.001
Population growth (σ)	1	1.97	0.16	0.19
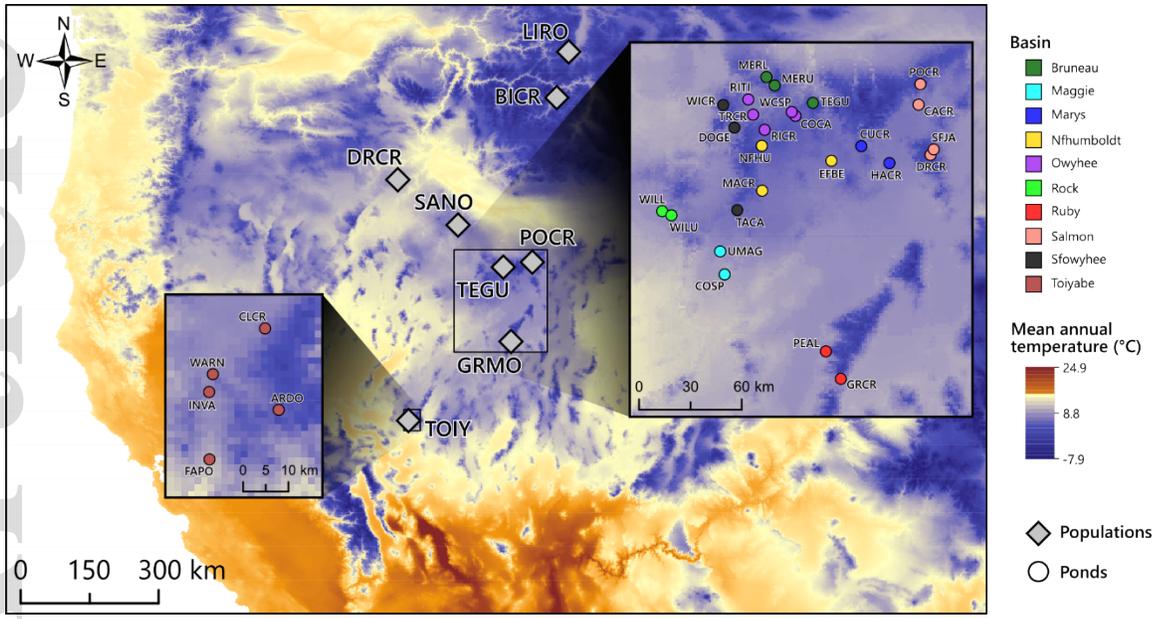
Fig.1. Map of the study area showing the eight in *R. luteiventris* populations surveyed using the capture-recapture method (grey diamonds) and the 31 breeding ponds (located in 10 hydrographic basins) considered in the genomic analyses. State lines were omitted for clarity; study sites occurred in Montana (LIRO), Idaho (BICR, SANO), Oregon (DRCR), and Nevada (POCR, TEGU, GRMO, TOIY).
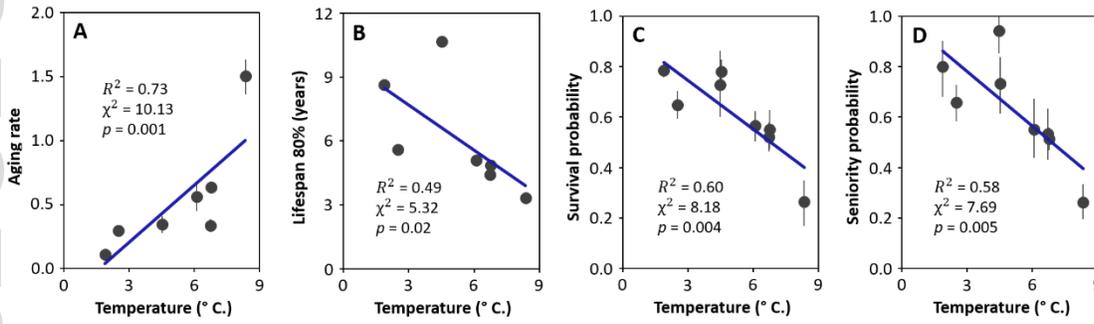
Fig.2. Influence of mean annual temperature (calculated for the period 1990-2019) on aging rate, lifespan 80% (age at which 80% of the individuals alive at the onset of adulthood die), mean annual adult survival probability, and mean annual seniority probability in *R. luteiventris*. Estimates (black points) and 95% credible intervals (error bars) extracted from Siler models (A and B) and Pradel models (C and D) are given. Siler model parameters appropriately converged for all populations except POCR; hence, aging rate and lifespan 80% of this population were not included in the analyses. We show the regression line (in blue) extracted from the linear models built to test the effect of temperature on demographic parameters. In addition, we provide R^2 and the statistics of the likelihood ratio tests (χ^2 and p).
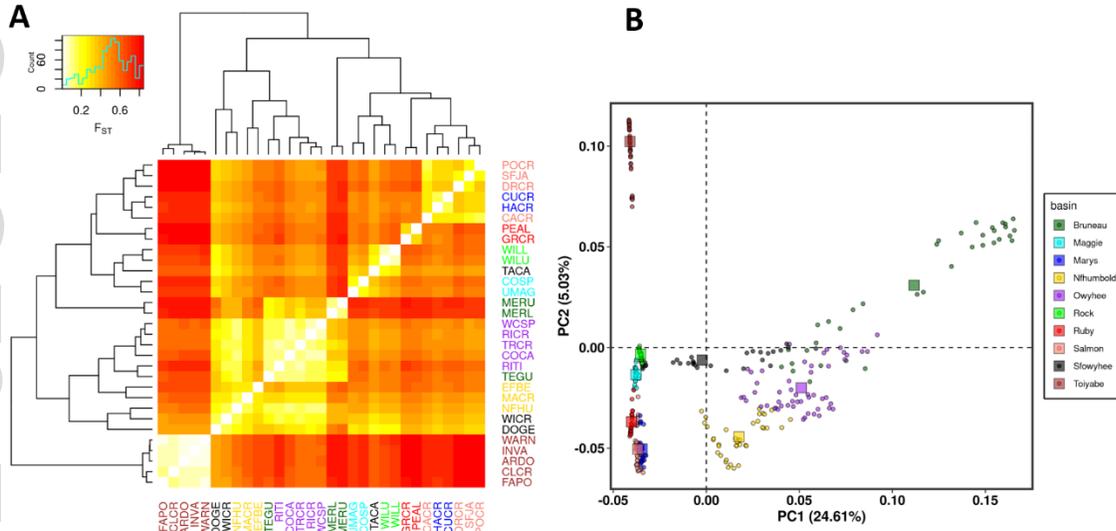
Fig.3. Population structure based on a F_{ST} matrix (A) and a Principal Component Analysis (B) in *R. luteiventris*. (A) Pairwise F_{ST} were calculated for each pair of breeding sites and were all significant (p-values are provided in **Supplementary material S1**, **Table S12**). Breeding sites (**Supplementary material S1**, **Table S2**) have been ordered based on a UPGMA cluster algorithm. (B) Principal Component Analysis represents the genetic variation within our SNP dataset. We colored the individuals according to their hydrographic basin of origin.
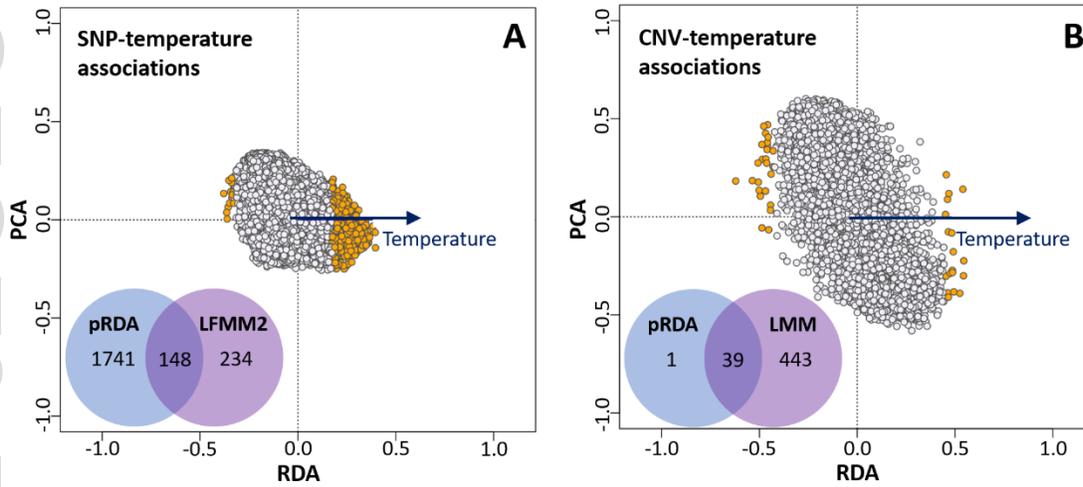
Fig.4. SNP-temperature (A) and CNV-temperature (B) associations using partial redundancy analyses (pRDA) in *R. luteiventris*. We also provide Venn diagrams showing the number of candidate SNPs and CNVs detected using either RDA, or latent factor mixed models (LFMM2), or both methods combined.
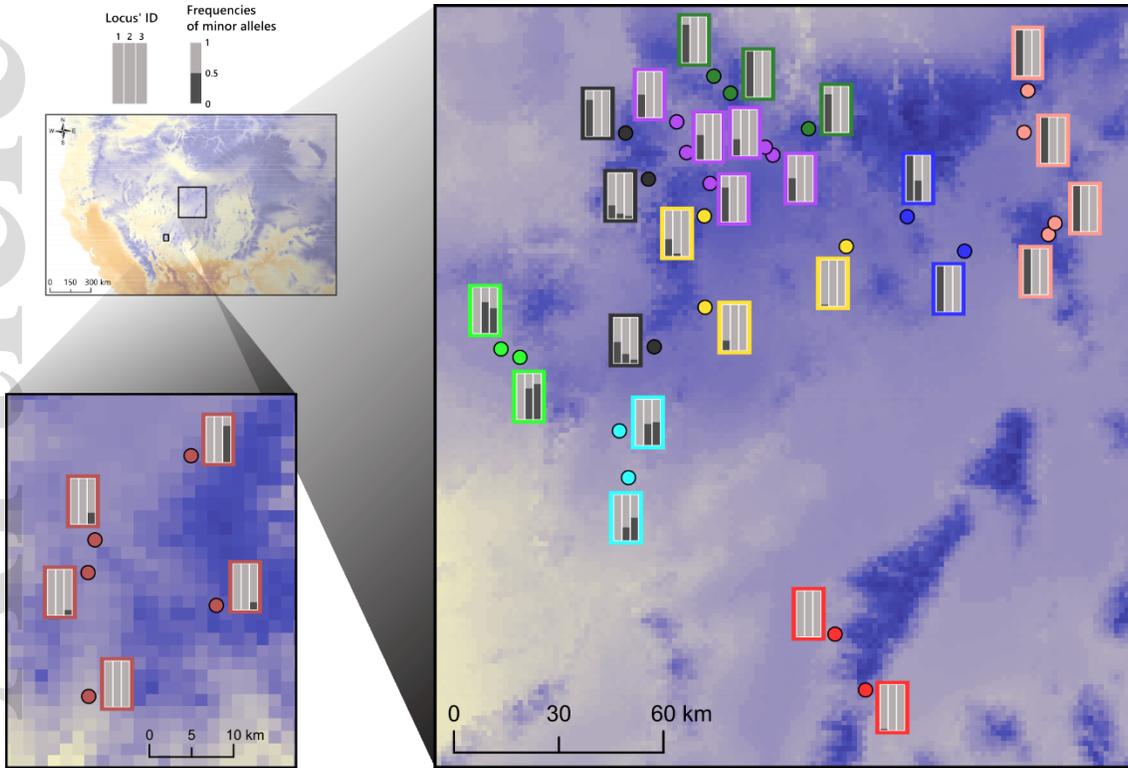
Fig.5. Minor allele frequency of three SNP candidates associated with temperature and located in protein-coding genes that could be involved in temperature-dependent life history variation observed in *R. luteiventris*: (1) locus 155392 is located within a gene regulating resistance to cold and anoxia, (2) locus 120066 within the gene regulating gonadotropin-releasing hormone receptor activity, and (3) locus 2796132 within the gene regulating the bradykinin production.
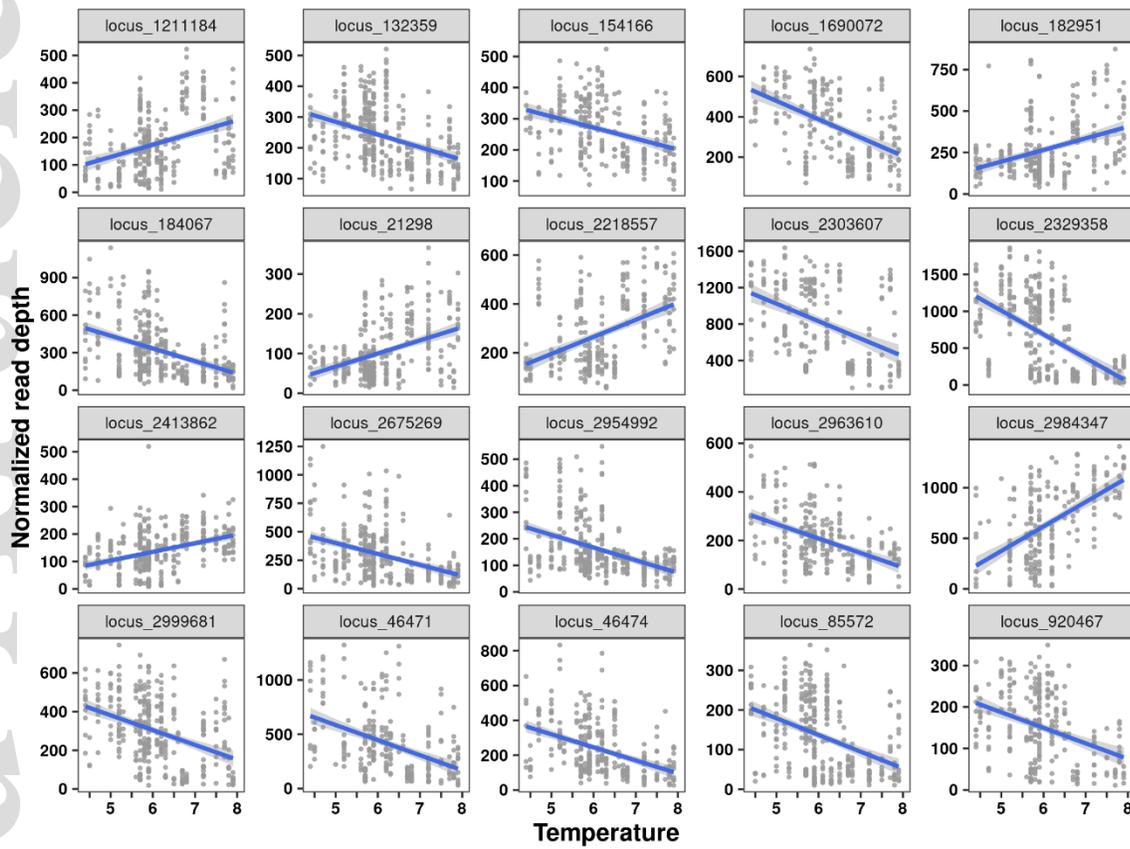
Fig.6. CNV-temperature associations in *R. luteiventris*: relationships between the normalized read depth and mean annual temperature for the 20 strongest CNV candidates (i.e., those with the high R²).